NANO MICRO small

Supporting Information

for *Small,* DOI: 10.1002/smll.201801131

Circulating Tumor Cell Phenotyping via High-Throughput Acoustic Separation

Mengxi Wu, Po-Hsun Huang, Rui Zhang, Zhangming Mao, Chuyi Chen, Gabor Kemeny, Peng Li, Adrian V. Lee, Rekha Gyanchandani, Andrew J. Armstrong, Ming Dao, Subra Suresh, and Tony Jun Huang**

Supporting Information

Circulating Tumor Cell Phenotyping *via* High-Throughput Acoustic Separation

Mengxi Wu, Po-Hsun Huang, Rui Zhang, Zhangming Mao, Chuyi Chen, Gabor Kemeny, Peng Li, Adrian V. Lee, Rekha Gyanchandani, Andrew J. Armstrong, Ming Dao, Subra Suresh, and Tony Jun Huang**

Supplementary Note 1:

Working Mechanism of the Hybrid PDMS-Glass Resonator Design

To enhance the acoustic energy density within the microchannel and to improve the throughput of the acoustic separation device, we employed a PDMS-glass hybrid channel to form an acoustic enclosure. Within this hybrid enclosure, the horizontal displacement of the surface parallel to the piezoelectric substrate which generates the Rayleigh waves is cancelled, and only the vertical displacement component will propagate leaky acoustic waves into the fluid (Figure 2(A)). The leaky waves travel in the fluidic domain and encounter the water-PDMS interface. The acoustic impedances of the water and PDMS are ~ 1.49 MPa·s/m and 0.98 MPa·s/m, respectively. The reflection coefficient $R_{water\text{-}PDMS}$ is calculated as:

$$R_{water-PDMS} = \left(\frac{Z_{PDMS} - Z_{water}}{Z_{PDMS} + Z_{water}}\right)^2 = 0.04$$

Only 4% of the acoustic energy is reflected back to the channel, while the vast majority is absorbed by the PDMS. Considering that the attenuation coefficient of PDMS is 3.3457 dB/MHz.cm, which is thousands of times higher than that of water (0.002 dB/MHz.cm), most of the acoustic energy transmitting into the PDMS is dissipated and wasted.

In order to reduce this energy loss, we embedded a thin glass layer (130 µm in thickness) at the top of the microchannel. Glass has a much larger acoustic impedance (~ 12 MPa·s/m) than PDMS and water. The reflection coefficients of the water-glass interface and the glass-PDMS interface are 0.61 and 0.72, respectively. Therefore, the reflected acoustic energy is increased to 89%. With the use of a hybrid PDMS-glass channel as a resonator, the acoustic energy that is enclosed within the fluidic domain is increased dramatically compared with the original PDMS channel.

Supplementary figures

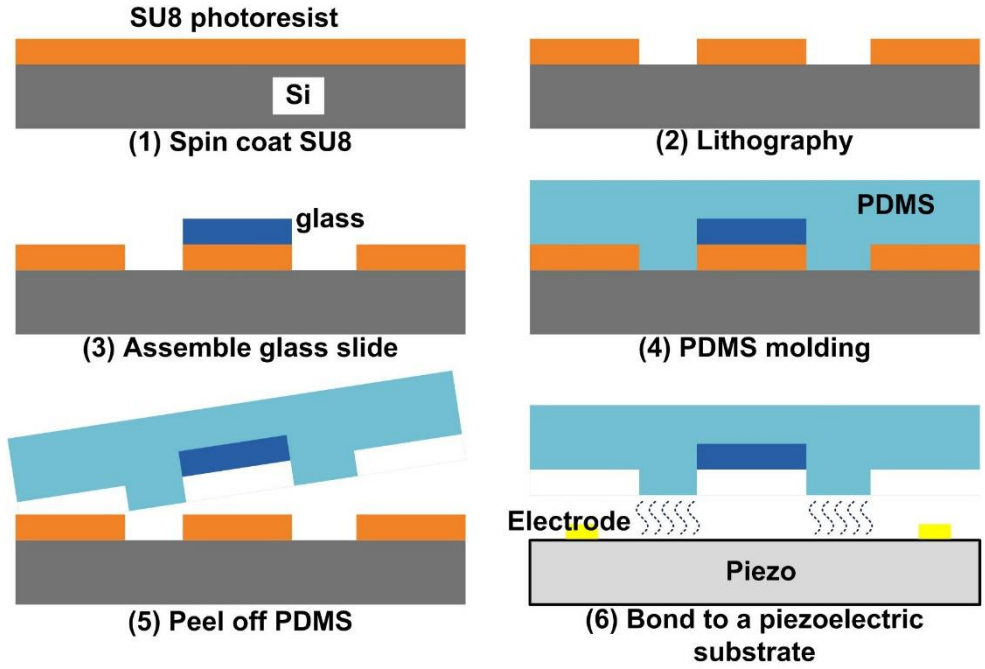

Figure S1. Fabrication process of the PDMS/glass hybrid channel for the high-throughput, acoustic-based separation device.

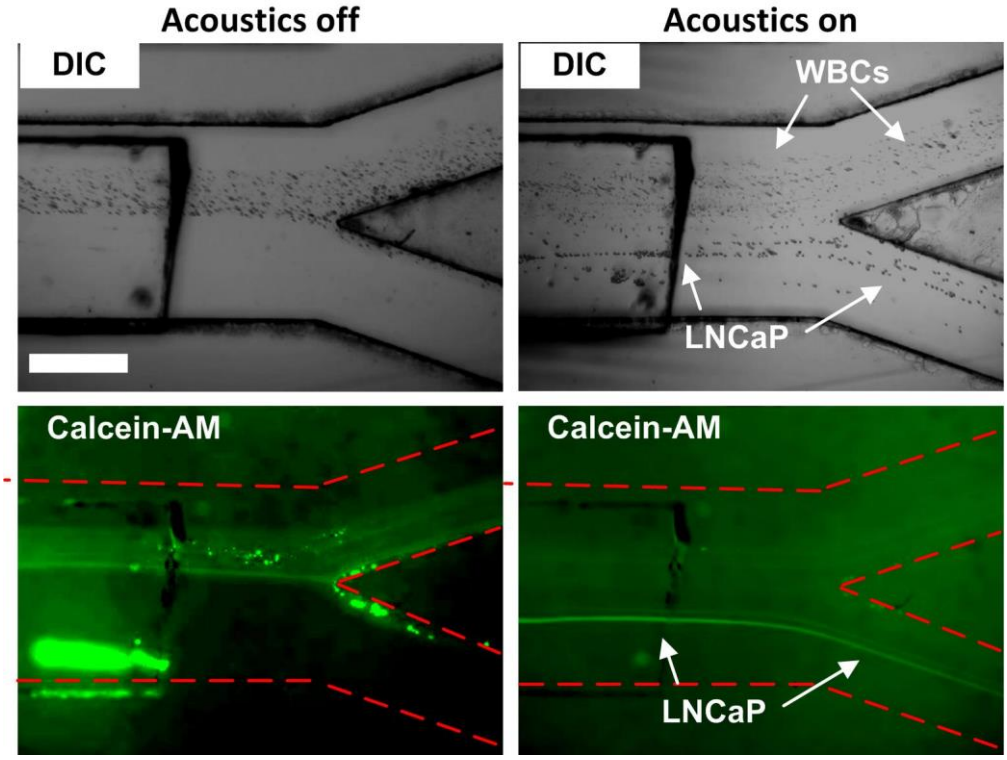

Figure S2. Acoustic separation of spiked LNCaP cells from WBCs. LNCaP cells were stained by Calcein-AM and mixed with 1 mL WBCs at a ratio of 1:4. When the acoustic wave was activated, LNCaP cells were pushed toward the bottom outlet by the acoustic field. WBCs were not pushed as far as LNCaP cells, only to the top outlet. Scale bar: 500 μm.

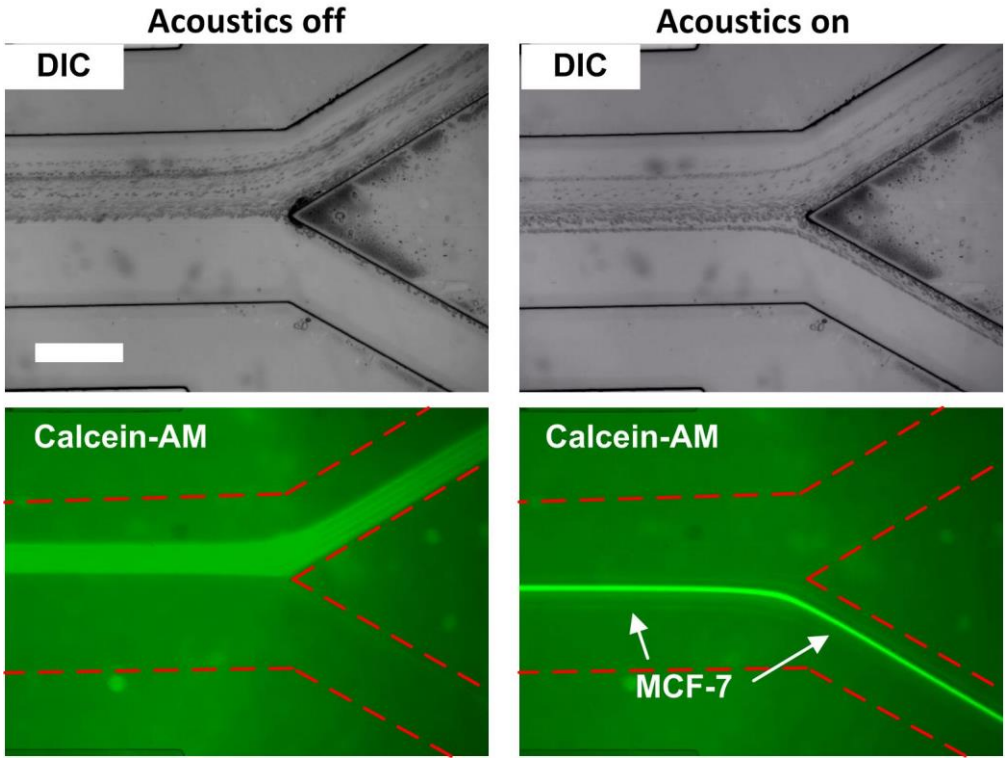

Figure S3. Acoustic separation of spiked MCF7 cells from WBCs. MCF7 cells were stained by Calcein-AM and mixed with 1 mL WBCs at a ratio of 1:10. When the acoustic wave was activated, MCF7 cells were pushed toward the bottom outlet by the acoustic field. WBCs were not pushed as far as MCF7 cells, only to the top outlet. Scale bar: 500 μm.

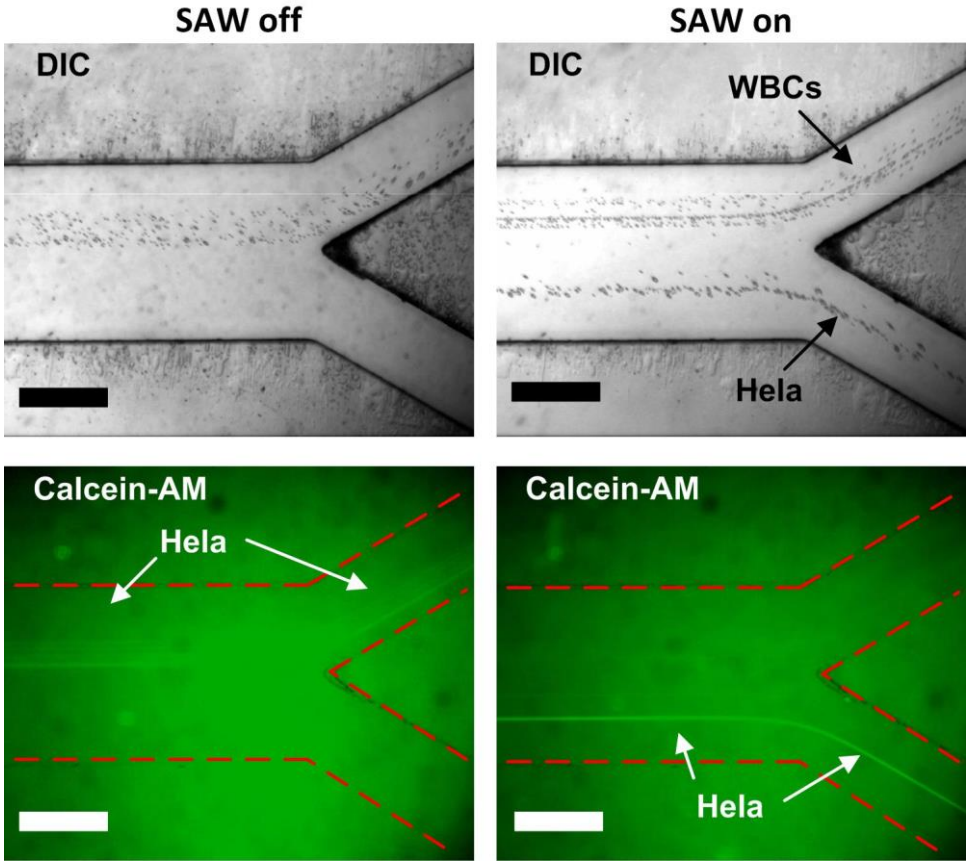

Figure S4. Acoustic separation of spiked Hela cells from WBCs. Hela cells were stained by Calcein-AM and mixed with 1 mL WBCs at a ratio of 1:10. Scale bar: 500 μm.

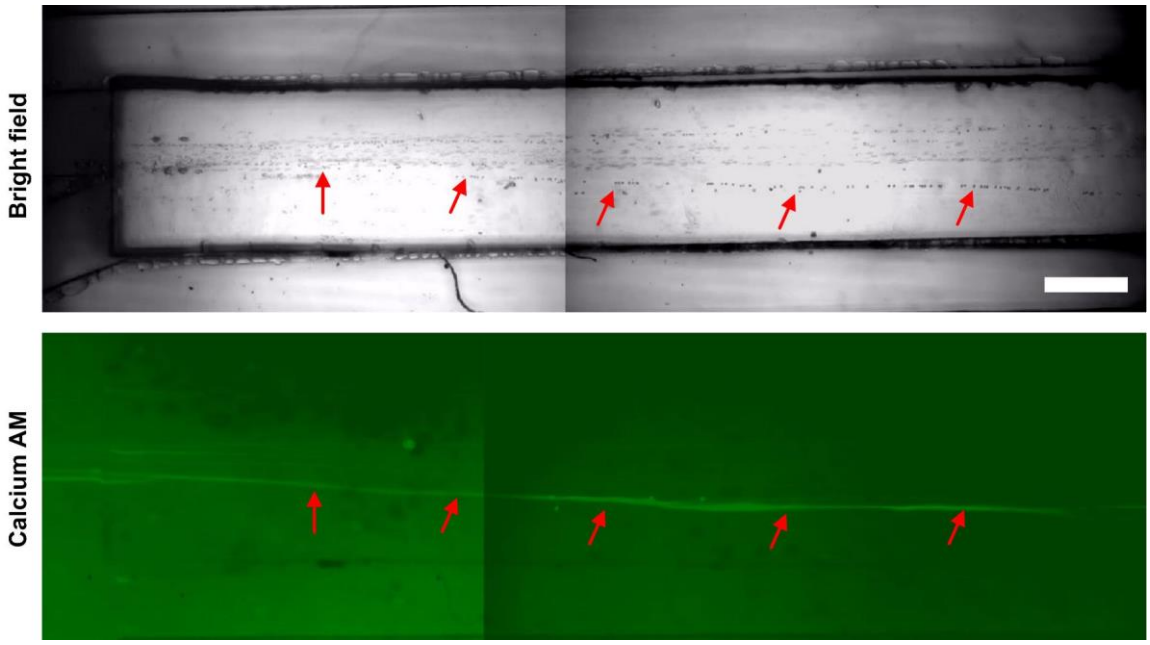

Figure S5. Deflection of cancer cells in the standing acoustic field formed by IDTs and PDMS/glass hybrid channel. Scale bar: 400 µm.

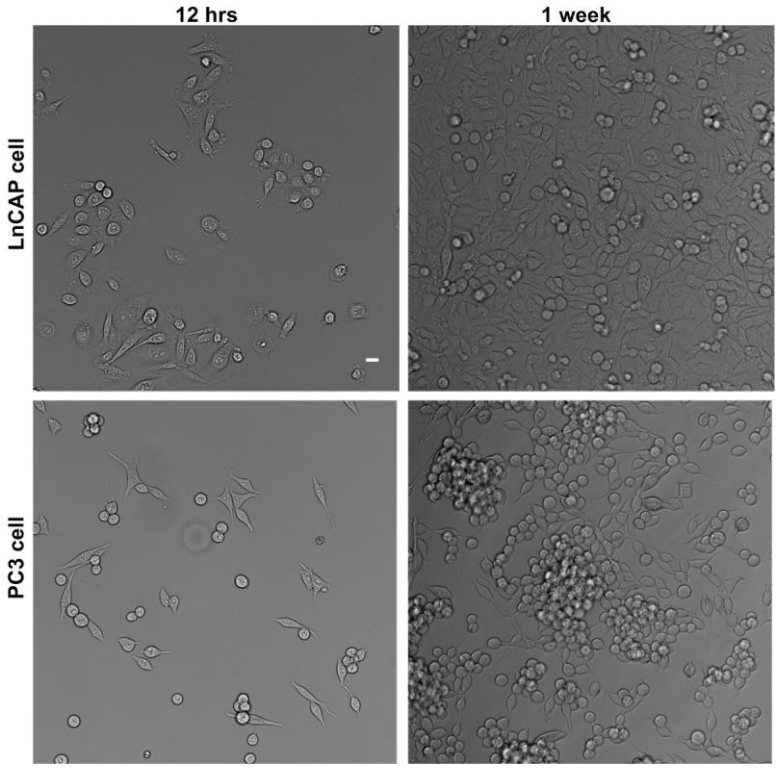

Figure S6. Long-term culture of isolated PC-3 and LNCaP cancer cell line shows the cancer cells are viable and able to proliferate after acoustic separation. Cancer cells were spiked into 1 mL WBCs. The mixture was processed through the high-throughput acoustic separation platform. After separation, cancer cells were collected from the sample outlet and cultured in Petri dishes. The conditions of

cells were monitored under microscope daily. The cancer cells start to attach during the first day. After one week, the cells still proliferated. Scale bar: 20 µm.

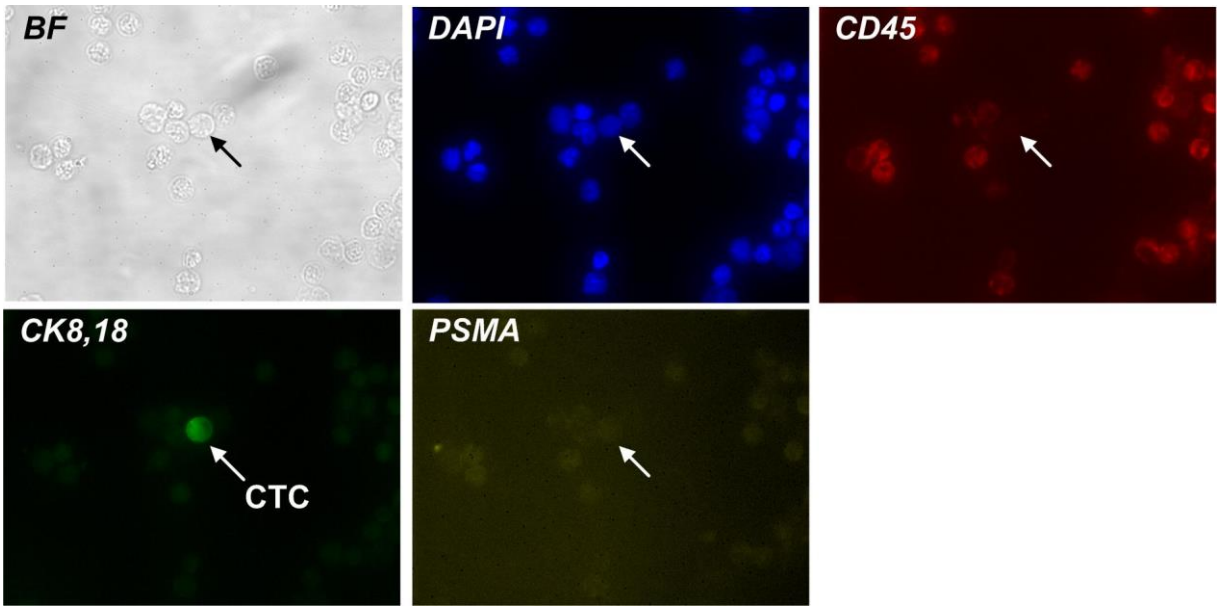

Figure S7. Identification of CTCs by immunostaining. The isolated cells from prostate cancer patient sample were stained by DAPI, CD45, CK8,18 and PSMA. The cells were identified under fluorescent microscope. The CTCs were featured as DAPI+/CD45-/CK8,18+.

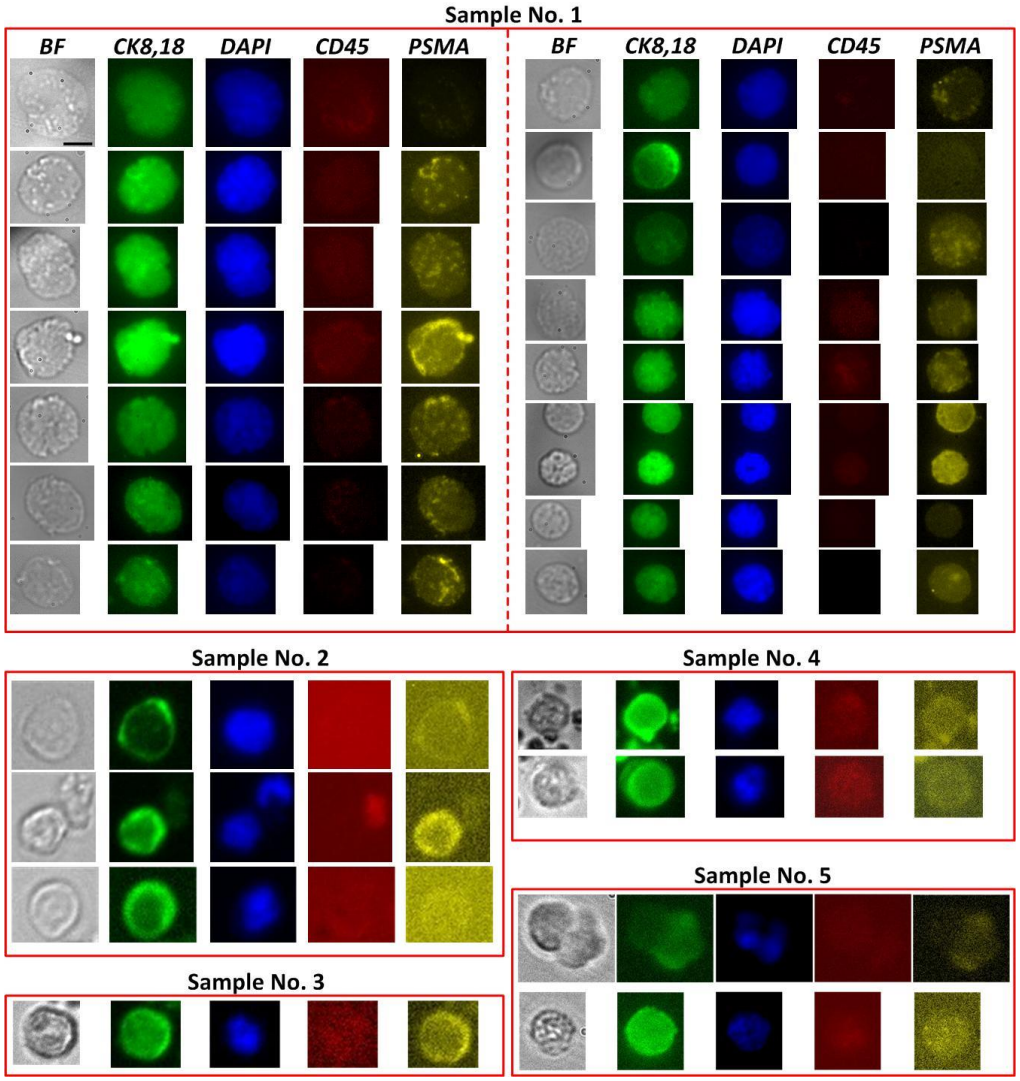

Figure S8. Selected images of CTCs isolated from prostate cancer patients by our acoustic methods. BF: bright field images. Cells were identified by cytokeratin marker CK8,18 and pan-leukocyte marker CD45. DAPI was used to stain the cell nucleus. The immunostaining pattern of CTCs is regarded as CK8,18+/DAPI+/CD45-. PSMA (prostate-specific membrane antigen) expression level varied, showing the heterogeneity of CTCs. Scale bar: 10 μm.